Anal. Chem. **2005,** *77,* 5973−5981

Observation of Increased Ion Cyclotron Resonance Signal Duration through Electric Field Perturbations

Nathan K. Kaiser and James E. Bruce*

Department of Chemistry, Washington State University, Pullman Washington 99164-4630

Ion motion in Fourier transform ion cyclotron resonance mass spectrometry (FTICR-MS) is complex and the subject of ongoing theoretical and experimental studies. Two predominant pathways for the loss of ICR signals are thought to include damping of cyclotron motion, in which ions lose kinetic energy and radially damp toward the center of the ICR cell, and dephasing of ion coherence, in which ions of like cyclotron frequency become distributed out of phase at similar cyclotron radii. Both mechanisms result in the loss of induced ion image current in FTICR-MS measurements and are normally inseparable during time-domain signal analysis. For conventional ICR measurements which take advantage of ion ensembles, maximization of the ion population size and density can produce the desired effect of increasing phase coherence of ions during cyclotron motion. However, this approach also presents the risk of coalescence of ion packets of similar frequencies. In general, ICR researchers in the past have lacked the tools necessary to distinguish or independently control dephasing and damping mechanisms for ICR signal loss. Nonetheless, the ability to impart greater phase coherence of ions in ICR measurements will allow significant advances in FTICR-MS research by improving the current understanding of ICR signal loss contributions of dephasing and damping of ion ensembles, increasing overall time-domain signal length, and possibly, resulting in more routine ultrahigh resolution measurements. The results presented here demonstrate the ability to employ a high density electron beam to perturb electric fields within the ICR cell during detection of cyclotron motion, in an approach we call electron-promoted ion coherence (EPIC). As such, EPIC reduces ICR signal degradation through loss of phase coherence, and much longer time-domain signals can be obtained. Our results demonstrate that time-domain signals can be extended by more than a factor of 4 with the implementation of EPIC, as compared to conventional experiments with otherwise identical conditions. The application of EPIC has also been observed to reduce the appearance of peak coalescence. These capabilities are not yet fully optimized nor fully understood in terms of the complex physics that underlies the enhancement. However, the enhanced time-domain signals can result in improved resolution in frequency-domain signals, and as such, this result is important for more efficient utilization of FTICR-MS. High resolution and accurate mass analysis are prime motivating factors in the application of advanced FTICR technology. We believe the approach presented here and derivatives from it may have significant benefit in future applications of advanced FTICR technology.

Fourier transform ion cyclotron resonance (FTICR) mass spectrometry[1] is unique in its ability to measure the mass-to-charge ratios (m/z) of many different charged species simultaneously while providing high resolution and mass measurement accuracy. The high performance capabilities associated with FTICR mass spectrometry arise from the extended time period in which ion detection takes place and allow for unambiguous charge state determination of large multiply charged ions, accurate mass analysis of complex peptide mixtures, and interpretation of complex MS/MS spectra.[2−10] The ICR experiment starts by first trapping the ions in the ICR cell with an axial magnetic field and an electrostatic potential well. Ions of the same m/z are excited together and form a coherent ion cloud that has a single measurable cyclotron frequency. Excited ion clouds must remain coherent in cyclotron motion for an extended period of time to allow multiple period measurements. As the ion clouds traverse their cyclotron orbits, they induce oscillating current in the detection circuitry with oscillation frequencies that result from

* Corresponding author. Department of Chemistry, P.O. Box 644630, Washington State University, Pullman, WA 99164-4630. Phone: (509) 335-2116. Fax: (509) 335-8867. james_bruce@wsu.edu.

(1) Comisarow, M. B.; Marshall, A. G. *Chem. Phys. Lett.* **1974**, *25*, 282−283.
(2) Masselon, C.; Anderson, G. A.; Harkewicz, R.; Bruce, J. E.; Pasa-Tolic, L.; Smith, R. D. *Anal. Chem.* **2000**, *72*, 1918−1924.
(3) He, F.; Emmett, M. R.; Hakansson, K.; Hendrickson, C. L.; Marshall, A. G. *J. Proteome Res.* **2004**, *3*, 61−67.
(4) Bossio, R. E.; Marshall, A. G. *Anal. Chem* **2002**, *74*, 1674−1679.
(5) Kelleher, N. L.; Lin, H. Y.; Valaskovic, G. A.; Aaserud, D. J.; Fridriksson, E. K.; McLafferty, F. W. *J. Am. Chem. Soc.* **1999**, *121*, 806−812.
(6) Reid, G. E.; McLuckey, S. A. *J. Mass Spectrom.* **2002**, *37*, 663−675.
(7) Wigger, M.; Eyler, J. R.; Benner, S. A.; Li, W.; Marshall, A. G. *J. Am. Soc. Mass Spectrom.* **2002**, *13*, 1162−1169.
(8) Little, D. P.; Speir, J. P.; Senko, M. W.; O'Connor, P. B.; McLafferty, F. W. *Anal. Chem.* **1994**, *66*, 2809−2815.
(9) Lipton, M. S.; Pasa-Tolic, L.; Anderson, G. A.; Anderson, D. J.; Auberry, D. L.; Battista, J. R.; Daly, M. J.; Fredrickson, J.; Hixson, K. K.; Kostandarithes, H.; Masselon, C.; Markillie, L. M.; Moore, R. J.; Romine, M. F.; Shen, Y.; Stritmatter, E.; Tolic, N.; Udseth, H. R.; Venkateswaran, A.; Wong, K. K.; Zhao, R.; Smith, R. D. *Proc. Natl. Acad. Sci. U.S.A.* **2002**, *99*, 11049−11054.
(10) Shi, S. D. H.; Hendrickson, C. L.; Marshall, A. G. *Proc. Natl. Acad. Sci. U.S.A.* **1998**, *95*, 11532−11537.

10.1021/ac050606b CCC: $30.25
Published on Web 08/20/2005

the summation of all ion cyclotron frequencies. This detection process allows for simultaneous high resolution and mass measurement accuracy, as is detailed in many excellent review articles and books.[11−13] Other types of mass spectrometers besides FTICR mass spectrometers have also utilized this nondestructive detection technique.[14,15] Detection of ICR signals for extended periods of time allows multiple measurements of each m/z species and provides the foundation for the high-performance capabilities of FTICR-MS. In principle, the longer time period that ion signals are detected, the greater the possible resolution and mass measurement accuracy. Furthermore, the achievable sensitivity of FTICR-MS is also related to the length of the detectable sinusoidal signal. However, in practice, acquisition of long time-domain signals does not guarantee high performance measurements with FTICR-MS.

Several factors can affect higher performance measurements with FTICR-MS. Although resolution, mass accuracy, and sensitivity can all be increased with improved time-domain signal length, Coulombic interactions and inhomogeneities in the axial electrostatic trapping potentials can cause variations in the observed cyclotron frequency with time and space within the ICR cell. In a three-dimensional quadrupolar potential field, the ion cyclotron frequency is independent of the positions of the ion clouds in the ICR cell;[16] however, in most ICR cell designs, this ideal three-dimensional quadrupolar potential is not achieved, and the resulting nonquadrupolar trapping potentials may contribute to frequency drifts.[17,18] There have been many different trap geometries designed to minimize electric field inhomogeneity and achieve improved quadrupolar trapping potentials while also maintaining high excitation and detection efficiencies.[16,19−21] In addition, the space charge potential arising from Coulombic interactions among ion clouds may vary with time. For example, as the ion clouds relax back toward the center of the ICR cell through collisional damping, their Coulombic interactions increase due to the higher ion density experienced at smaller cyclotron radii. This increase in ion density may cause the observed cyclotron frequency to decrease, as discussed by Guan et al.[17] Therefore, conditions can arise within the ICR cell that decrease instrument performance and prevent extended periods of ion signal detection. To exploit the high performance capabilities of FTICR-MS in more routine fashion, these conditions must be minimized.

Two primary processes are currently thought to limit ions from being detected for extended periods of time. The combination of collisional damping[22] and dephasing of the ion packet causes the detected ICR signal to decay over time. Collisional damping is resultant from collisions between the ions and residual neutral gas molecules present in the ICR cell during detection of cyclotron motion. The coherent ion packet loses kinetic energy through these collisions. To maintain constant cyclotron frequency, the lower kinetic energy of the ions results in a smaller cyclotron orbit. As such, the ions become farther away from the detection plates, and the observed signal is decreased. Ion/neutral collisions are the primary reason that ICR measurements are normally carried out under ultralow-pressure conditions. There are two limiting forms of collisional damping: an ion-induced dipole (Langevin) collision model, leading to an equation of ion motion damping term that is linear in velocity, resulting in a Lorentzian frequency-domain line shape, and a hard-sphere collisional model, which produces a quadratic damping term.[22] The other primary mechanism for loss of ICR signal is dephasing. This process happens when the ion cloud loses its phase coherence, and ions of the same m/z value become distributed at varying cyclotron phase angles instead of remaining as a coherent ion packet. A number of different processes that contribute to ion cloud dephasing have been identified. For example, ion cloud density, magnetic field strength, Coulombic interaction with other ion clouds, total cloud charge, and ion velocity are all parameters that have an effect on dephasing.[23] As described by Peurrung and Kouzes, imposed shear effects disrupt the ion phase coherence and cause the ion cloud to be distributed at various cyclotron phase angles. These authors list possible sources of shear to include magnetic field inhomogeneities, image charge effects, passive space charge at the trap center, and nonharmonic or asymmetric components of the trapping potential well.[23] In addition, some ions present in the ICR cell may have sufficient energy to follow a trajectory that is different from that of the bulk ion cloud. For example, ions with velocities significantly different from that of the ion cloud are able to separate from the majority of ions which leads to a loss of detected ICR signal. As a result, the reduction of charge in the ion packet decreases coherence and induces a smaller image charge on the detection plates. Currently, there is no convenient way to determine the contribution of each signal loss mechanism to the observed signal decay; however, differentiation between damping and dephasing of cyclotron motion can be obtained through observation of multiple harmonics.[24−27] Normally, the observed decay in the time-domain signal is considered to be some combination of collisional damping and dephasing.

Efforts have been made to minimize damping and dephasing of ion cyclotron motion.[7,10,28,29] There are also examples in which ion dephasing has been completely eliminated, such as demon-

(11) Marshall, A. G.; Hendrickson, C. L.; Jackson, G. S. *Mass Spectrom. Rev.* **1998**, *17*, 1−35.
(12) Marshall, A. G.; Hendrickson, C. L. *Int. J. Mass Spectrom.* **2002**, *215*, 59−75.
(13) Alan G. Marshall; Verdun, F. R. *Fourier Transforms in NMR, Optical, and Mass Spectrometry: A User's Handbook*; Elsevier Science Publishers: New York, 1990.
(14) Benner, W. H. *Anal. Chem.* **1997**, *69*, 4162−4168.
(15) Makarov, A. *Anal. Chem.* **2000**, *72*, 1156−1162.
(16) Guan, S.; Marshall, A. G. *Int. J. Mass Spectrom. Ion Processes* **1995**, *146/147*, 261−296.
(17) Guan, S.; Wahl, M. C.; Marshall, A. G. *Anal. Chem.* **1993**, *65*, 3647−3653.
(18) Bruce, J. E.; Anderson, G. A.; Hofstadler, S. A.; Winger, B. E.; Smith, R. D. *Rapid Commun. Mass Spectrom.* **1993**, *7*, 700−703.
(19) Ostrander, C. M.; Arkin, C. R.; Laude, D. *J. Am. Soc. Mass Spectrom.* **2001**, *12*, 30−37.
(20) Guan, S.; Marshall, A. G. *Rev. Sci. Instrum.* **1995**, *66*, 63−66.
(21) Bruce, J. E.; Anderson, G. A.; Lin, C.-Y.; Gorshkov, M.; Rockwood, A. L.; Smith, R. D. *J. Mass Spectrom.* **2000**, *35*, 85−94.
(22) Guan, S.; Li, G.-Z.; Marshall, A. G. *Int. J. Mass Spectrom. Ion Processes* **1997**, *167/168*, 185−193.
(23) Peurrung, A. J.; Kouzes, R. T. *Phys. Rev. E: Stat. Phys., Plasmas, Fluids, Relat. Interdiscip. Top.* **1994**, *49*, 4362−4368.
(24) Pan, Y. P.; Ridge, D. P.; Wronka, J.; Rockwood, A. L. *Rapid Commun. Mass Spectrom.* **1987**, *1*, 121.
(25) Pan, Y. P.; Ridge, D. P.; Rockwood, A. L. *Int. J. Mass Spectrom. Ion Processes* **1988**, *84*, 144.
(26) Nikolaev, E. N.; Gorshkov, M. V.; Mordehai, A. V.; Talrose, V. L. *Rapid Commun. Mass Spectrom.* **1990**, *4*, 144.
(27) Grosshans, P. B.; Marshall, A. G. *Int. J. Mass Spectrom. Ion Processes* **1991**, *107*, 49−81.
(28) Gordon, E. F.; Muddiman, D. C. *J. Mass Spectrom.* **2001**, *36*, 195−203.
(29) Stults, J. T. *Anal. Chem.* **1997**, *69*, 1815−1819.

strated with single or individual ion measurements.[30−35] In those experiments, a single ion carried enough charge that it produced a detectable image current. Single ion measurements are unique in that there is no need for phase coherence between ions, since only one ion of a specific m/z is present. In those cases, the only signal loss mechanism other than through reaction, is through collisional damping. This earlier work[36] demonstrated a significant improvement in time-domain signal length, as compared to the conventional ion ensemble detection scheme. In single ion experiments, measurements were conducted with species of the same molecular weight and under similar vacuum conditions. Thus, increased time-domain signals could be attributed to the removal of dephasing mechanisms. However, most ions do not carry enough total charge to be detected as single ions. In most conventional detection methods, an ensemble of ions is needed to supply enough charge to induce a detectable image current. Ions of exactly the same m/z are excited in-phase with each other. These ions form a stable ion packet, and their collective charge induces a measurable image current for detection. These ion packets seem to be more stable as the number of charges in the ion packets increase. Ion cloud stability is important, since it prevents dephasing; however, it can also be limited by a number of factors. Peurrung and Kouzes[23] presented an explanation for the underlying foundation of long term ion cloud stability. Nikoleav et al. have recently presented numerical simulations with a higher degree of accuracy and give a more revealing model of the complex ion motion in the ICR cell.[37] The discussion by Peurrung and Kouzes pointed out that the ion cloud undergoes an additional rotational motion separate from cyclotron and magnetron motion. The ion cloud generates its own electric field, and in the presence of a magnetic field, the ion cloud rotates about its own center. Ion cloud rotation counterbalances shear factors mentioned above that can tear the ion cloud apart. Ion cloud rotation is thought to be the primary basis that makes the duration of long time-domain signals possible for an ensemble of ions. This ion cloud spin rotation increases cloud stability as a function of higher charge density. However, the number of ions that can form an ion cloud and still retain the resolving power necessary to separate closely spaced peaks is limited by phase-locking or ion cloud coalescence. Mitchell and Smith[38] reported that this coalescence phenomenon occurs when ion clouds have similar cyclotron frequencies and large Coulombic charges. As the Coulombic charge in the ion clouds increase, there is an increased likelihood that ion clouds with similar, but not identical cyclotron frequencies will begin to rotate around each other. These separate ion clouds can phase-lock and continue on a cyclotron orbit at a mutual cyclotron frequency and will appear as one peak in the mass spectrum. Thus, mitigation of ion cloud dephasing through increased ion cloud density requires careful control to avoid conditions that promote phase-locking or coalescence.[29] These two opposing constraints, namely, the ability to trap enough ions to promote single m/z ion cloud stability during detection while keeping the ion population small enough to avoid coalescence represent real, fundamental limitations of FTICR-MS performance.

Increased time-domain signal length can provide improved resolution and mass measurement accuracy, and as such, increased routine time-domain signal acquisition length is a goal of many studies to advance FTICR-MS technology. However, ion motion in the ICR cell is still not completely understood, and improved comprehension of ion motion could result from methods that decouple collisional damping and dephasing signal loss mechanisms. The primary motivation of the present manuscript is to report the observation of experimental effects that serve to reduce ion cloud dephasing mechanisms. We call the observed effect electron-promoted ion coherence, or EPIC, since, with the application of a high density electron beam during detection, we observed significant improvement in the length of detected coherent cyclotron motion. Electron beams have been previously introduced into the ICR detection cell for a number of different reasons, such as ionization, dissociation,[39] ion transfer,[40] and ion trapping (EBIT).[41] However, to the best of our knowledge, this is the first time that the electron beam has been used to modulate electric fields during detection of cyclotron motion. To the best of our ability to determine, the effects described below appear to result in decreased ion cloud dephasing and result in significantly improved time-domain signal length. Also to the best of our knowledge, this capability represents an entirely new tool that can be used to improve FTICR-MS performance as well as help distinguish the two primary signal loss mechanisms. For example, this decoupling could enable a better understanding of ion motion and phase coherence, which ultimately enables improved detection techniques that enhance resolution, mass measurement accuracy, and sensitivity.

EXPERIMENTAL SECTION

Ubiquitin (MW_{avg} = 8565 Da), bradykinin (MW_{avg} = 1060 Da), and substance P (MW_{avg} = 1348 Da), obtained from Sigma Aldrich, were dissolved and diluted to 10 μM concentration with a solution of 49:49:2 by volume of water, methanol, and acetic acid. The experiments were performed with a Bruker Daltonics Apex-Q 7-T FTICR mass spectrometer. The instrument has a mass selective quadrupole, which allows for mass-selective accumulation of a specific m/z species. Electrospray was used as the ionization source in which the voltage on the capillary was set between −1800 and −2000 V. A syringe pump was used to introduce solutions at a rate of 15−25 μL/h. Ions were trapped in the ICR

(30) DiFilippo, F.; Natarajan, V.; Bradley, M.; Palmer, F.; Pritchard, D. E. *Phys. Scr., T* **1995**, *T59*, 144−154.
(31) Bruce, J. E.; Cheng, X.; Bakhtiar, R.; Wu, Q.; Hofstadler, S. A.; Anderson, G. A.; Smith, R. D. *J. Am. Chem. Soc.* **1994**, *116*, 7839−7847.
(32) Smith, R. D.; Cheng, X.; Bruce, J. E.; Hofstadler, S. A.; Anderson, G. A. *Nature (London, U.K.)* **1994**, *369*, 137−139.
(33) Cheng, X.; Camp, D. G., 2nd; Wu, Q.; Bakhtiar, R.; Springer, D. L.; Morris, B. J.; Bruce, J. E.; Anderson, G. A.; Edmonds, C. G.; Smith, R. D. *Nucleic Acids Res.* **1996**, *24*, 2183-2189.
(34) Cheng, X.; Bakhtiar, R.; Van Orden, S.; Smith, R. D. *Anal. Chem.* **1994**, *66*, 2084−2087.
(35) Chen, R.; Cheng, X.; Mitchell, D. W.; Hofstadler, S. A.; Wu, Q.; Rockwood, A. L.; Sherman, M. G.; Smith, R. D. *Anal. Chem.* **1995**, *67*, 1159−1163.
(36) Bruce, J. E.; Anderson, G. A.; Udseth, H. R.; Smith, R. D. *Anal. Chem.* **1998**, *70*, 519−525.
(37) Nikolaev, E. N.; Popov, A. M.; Heeren, R. M. A.; Sharova, M. S.; Pozdneev, A. V.; Chingin, K. S.; Taban, I. M. 53rd ASMS Conference, San Antonio, TX, June 5−9, 2005.
(38) Mitchell, D. W.; Smith, R. D. *Phys. Rev. E. Stat. Phys., Plasmas, Fluids, Relat. Interdiscip. Top.* **1995**, *52*, 4366−4386.
(39) Zubarev, R. A.; Kelleher, N. L.; McLafferty, F. W. *J. Am. Chem.ical Soc.* **1998**, *120*, 3265−3266.
(40) Hendrickson, C. L.; Hadjarab, F.; Laude, D. A., Jr. *Int. J. Mass Spectrom. Ion Processes* **1995**, *141*, 161−170.
(41) Beiersdorfer, P.; Becker, S.; Beck, B.; Elliott, S.; Widmann, K.; Schweikhard, L. *Nucl. Instrum. Methods Phys. Res., Sect. B* **1995**, *98*, 558−561.

cell using Sidekick.[42] In select experiments, argon was pulsed into the ICR cell to cool the ions, followed by a 2−4 s delay for pump down time before excitation of ion cyclotron motion. Experiments that utilized argon cooling gas are indicated below. In all experiments, the ion-gauge reached a minimum value of 5×10^{-10} Torr before the ions were excited. The projected pressure in the cell may be up to an order of magnitude higher. EPIC experiments were performed by supplying a high-density beam of electrons through the center of the ICR cell during the detection event. The electron beam was produced using a hollow cathode emitter[43] normally used for electron capture dissociation (ECD) experiments.[39,44,45] The cathode emitter is located outside the ICR cell and is positioned along the central axis of the ICR cell. The cathode has an outer diameter of 7.6 mm and an inner diameter of 3.5 mm and was heated by passing a current of 1.5 A through it using an external power supply. The pulse sequence of the experiment was modified so that the electron beam was initiated after the cyclotron excitation event and before the detection event. The electrons were pulsed into the ICR cell under conditions similar to those used with ECD, except that the timing of the pulse sequence was different from normal ECD experiments. The electron emitter was continually heated throughout all phases of the experiment. The bias applied to the emitter was set at 0.0 V for no electron beam, and between −0.1 and −1.3 V to stimulate emission of electrons. This high-density beam of electrons was continuously produced during the entire length of the detection event. In EPIC experiments, the electron beam was turned on only after ions reached their excited cyclotron orbits and was turned off after the termination of the detection event. Experiments were performed in narrow-band detection mode for ultrahigh resolution and acquisition of longer attainable time-domain signals. Isolation of specific charge states was performed prior to the ions entering the ICR cell with the mass-selective quadrupole. Xmass (version 7.0.6) was used as the data acquisition software. All data sets were collected as single scans. Control, or normal, time-domain signals shown for comparison were obtained by applying 0.0 V bias to the emitter; during the subsequent EPIC experiment, a voltage bias of −0.1 to −1.3 V was applied to the emitter to produce the high-density electron beam. No other parameters were changed between experiments. ICR-2LS [46] was used for data processing. The substance P data set was apodized (Welch) and zero-filled once before obtaining the mass spectrum. The measurements of cyclotron frequency drift with time were obtained using the "Sweep" [18] program, written as a module within ICR-2LS.

RESULTS AND DISCUSSION

A high-density, low-energy electron beam produced along the central axis outside the ICR cell during detection of ion cyclotron motion was found to significantly increase the length of the observed time-domain signal. Though the dispenser cathode used to create the electron beam was installed to produce electrons for ECD, no fragmentation resultant from the electron beam was observed during EPIC experiments. The ion cloud and electron beam likely have no overlap during detection, since the ion cloud is at a larger cyclotron orbit as its motion is being detected. The calculated post excitation ICR orbital radius was ∼1.8 cm, determined through single frequency excitation experiments. Furthermore, if the electron beam and the excited ion cloud were to intersect during detection, the resultant ECD fragment ions, if formed, would likely be distributed out of phase with each other at similar radii, and little or no observable signal would have been detected. With the present EPIC approach, the electron beam is turned on only after the ions have been promoted to their excited cyclotron radius. As mentioned above, this process is different from what normally occurs for ECD, in which the electrons are pulsed into the ICR cell with the sole purpose of interacting with the parent ions to cause fragmentation. It should be noted that ECD experiments performed with application of electron beams of similar density and duration result in complete loss of all observed ion signals. For ECD experiments, the electron pulse is initiated for a short time period, fragmentation takes place, and the resulting ions are excited and detected.

We originally investigated the use of the electron beam on ion cyclotron motion in an attempt to learn about electrostatic field effects on ion cyclotron frequencies. Previous publications reported the observation and correction of cyclotron frequencies drifts during signal acquisition.[17,18] Since many of these efforts ascribe measured cyclotron frequency shifts to electrostatic field effects on cyclotron motion, we anticipated the high-density electron beam produced from the ECD dispenser cathode would prove to be a useful tool to investigate these affects.

However, a very striking and unexpected result was observed from the initial experiments, which was a substantial increase in time-domain transient length. The initial observation of increased time-domain transient length with the electron beam was carried out using bradykinin with conditions that were not optimized for long-time domain signal acquisition. Bradykinin ions were trapped in the ICR cell using Sidekick, which is thought to cause the ions to have slight magnetron motion and to be slightly more spatially distributed in the ICR cell.[42] In addition, no collision gas was added for ion cooling and compression of trapped ions before excitation. The initial observed result is illustrated in Figure 1, which shows both the traditional time-domain signal and the initial EPIC results along with their corresponding mass spectra. As mentioned above, the initial non-EPIC results shown here were acquired without prior optimization of conditions that enable long time-domain signal acquisition and, thus, are not representative of what one might expect in terms of longer time-domain transient performance from this type of instrument. However, initial application of EPIC resulted in improvement in the observed time-domain signal length, even for these nonideal conditions. The striking feature here of significant interest to us was the unexpected increase in time-domain signal length.

The observation of increased signal duration during the electron beam application was surprising to us for several reasons. First, ICR signal detection was not precluded from noise or disrupted ion phase coherence caused by pulsing the dispenser cathode during detection. One might expect that, given the small signals resultant from ion motion and the extremely high sensitivity of the detection circuitry normally used with FTICR-MS, signal

(42) Caravatti, P.; Allemann, M. *Org. Mass Spectrom.* **1991**, *26*, 514−518.
(43) Tsybin, Y. O.; Witt, M.; Baykut, G.; Kjeldsen, F.; Hakansson, P. *Rapid Commun. Mass Spectrom.* **2003**, *17*, 1759−1768.
(44) Zubarev, R. A. *Mass Spectrom. Rev.* **2003**, *22*, 57−77.
(45) Sze, S. K.; Ge, Y.; Oh, H.; McLafferty, F. W. *Proc. Natl. Acad. Sci. U.S.A.* **2002**, *99*, 1774−1779.
(46) Anderson, G. A.; Bruce J. E.; Smith R. D. 2.18 ed.: Richland, WA, 1996.

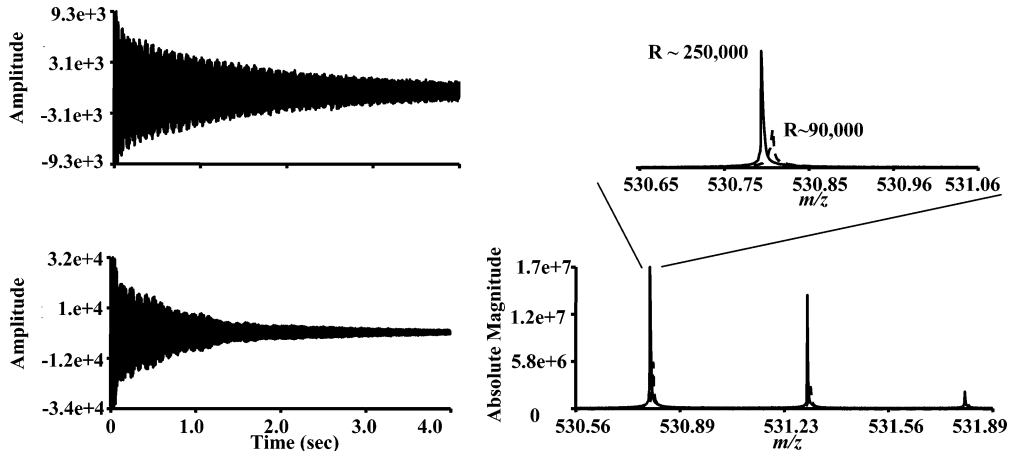

Figure 1. Our initial observation of EPIC is shown with successive time-domain signals of bradykinin $[M + 2H]^{2+}$: (a) with no modification to the detection scheme and (b) EPIC time-domain signal. The EPIC results extend well past the collected 4 s. The resultant mass spectra obtained from the time-domain signal are also shown.

detection might be much more difficult with the electron beam turned on. Second, one might consider that changes in the electrostatic field inside the ICR cell might disrupt all coherent ion motion due to the previous discussion of cloud stability and electrostatic field-induced shear effects. These data suggest, at least under a range of conditions that were investigated, that this is not the case. In fact, the ICR signal appears more stable under EPIC conditions.

We believe that this observation of increased time-domain signal length has significance, and our initial results warranted further investigation. Therefore, the next experiments were performed to see if we could obtain a similar increase in ICR signal duration under conditions that were more amenable to longer time-domain signals with conventional or non-EPIC experiments. The conditions in the ICR cell were slightly modified from those applied for the experiments discussed above by pulsing argon gas into the ICR cell to cool the ions and reduce axial oscillation after trapping but prior to cyclotron excitation. This approach is similar to those used in most labs to acquire longer time-domain signals, since reduction of axial motion results in a more compact ion cloud and the opportunity to work at lower trapping potentials, which seem more suitable to longer time-domain signal detection. Figure 2a shows the resultant time-domain signal from the narrow-band detection of ubiquitin $[M + 7H]^{7+}$. All parameters in the experiment were carefully adjusted and controlled to maximize the observed time-domain signal length. This resulted in detectable signal for ~25 s, and this result represents the best we could achieve with the normal detection method on that particular day. The subsequent time-domain signal was acquired immediately following, using exactly the same experimental parameters as were used in Figure 2a, with the exception of the application of the electron beam. The results are shown in Figure 2b. With EPIC, the length of the observed time-domain signal increased to over 70 s. This observation was very exciting, since it demonstrated that significantly improved ion signal duration could be achieved with EPIC, even when carefully optimized conditions were implemented prior to EPIC. We were still able to observe the same significant improvement in time-domain signal length as we observed without careful tuning and cooling of axial motion. With the application of EPIC, the time-duration that signal could be detected was enhanced by a factor of ~3.

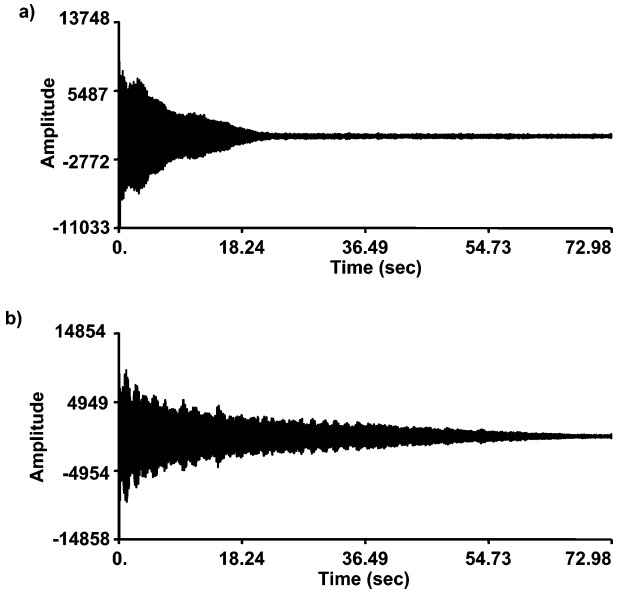

Figure 2. Successive time-domain signals for the ubiquitin $[M + 7H]^{7+}$. (a) With no modification to the detection scheme, there is signal duration for approximately 25 s. (b) With the EPIC experiment, there is signal duration for over 70 s. There is improvement by a factor ~3 with the application of EPIC.

As mentioned above, ICR signal loss is a convoluted combination of collisional damping and dephasing. Collisional damping occurs when the ion packet collides with neutral molecules in the ICR cell. Therefore, with higher pressure in the ICR cell, we would expect to see shorter time-domain signals. In our experiments, the pressure in the ICR cell during signal acquisition was the same, to the best of our ability to measure it. Since the only difference was the application of the electron beam, one might consider the effects of the electron beam on the effective pressure in the ICR cell. Pressure changes associated with the activation of the electron beam are likely small, if any, on the basis of the lack of any measured changes observed with the ion gauge. In addition, any negative change in pressure, as would be needed to ascribe the observed increase in performance with EPIC to changes in collisional damping rates, seems highly unlikely, given the low energy of the electrons and the low base pressure measured on the system. That is, any possible "pumping" resultant

from electrons interacting with neutrals, producing ions that are effectively able to escape the trap and, thus, result in lower in-cell pressures, is unlikely due to the fact that the electron energies are well below the ionization energies of any possible neutral species that could be present in the cell. Instead, it seems more likely that if any change to the pressure were to occur as a result of the electron beam, it would likely be a shift to a higher pressure, resulting from the heating associated with the production of electrons from the dispenser cathode. This, too, is likely a very small contribution to the observations. Therefore, decay of signal amplitude resultant from collisional damping of the ion packet is expected to be approximately the same in both experiments. The calculated collision frequency between the ions and residual neutral molecules was ~2 collisions/s, on the basis of the cell pressure of $\sim 5 \times 10^{-9}$ Torr and an excitation radius of 1.8 cm. Thus, we suspect that electrostatic field effects and ion cloud coherence are much more likely the root of the observed enhancement in time-domain signal length and that application of a steady stream of electrons through the ICR cell reduces electrostatic factors that promote ion cloud dephasing.

As pointed out in several previous theoretical treatments of ion motion, the number of ions can significantly impact the stability of ion clouds and the length of detectable ICR signals. This factor was considered in these investigations, as well. The number of ions that make up the ion clouds in each experiment from Figure 2a and 2b was held constant to the best of our ability. Since the number of ions can be significantly altered with ionization, ion accumulation, injection, trapping, and excitation conditions, all parameters were held constant between EPIC and non-EPIC experiments. Furthermore, one thing to note in comparison of parts a and b of Figure 2 is that the initial amplitudes of the two time-domain signals are approximately the same. The initial amplitude is a function of the total charge in the ion packet and the radius to which the ions clouds are accelerated. The initial amplitudes of the time-domain signals shown in Figure 2 are the same within expected experimental error, indicating that the number of ions present in each experiment is very nearly the same. In addition to the application of the electron beam, no modification was performed to any other parameter in the experiment. As the number of ions in the ICR cell was decreased by reducing the ion accumulation time, the length of the detected transient signal also decreased with and without the application of EPIC. However, the same relative improvement in transient signal length was observed with the application of EPIC, even with reduced ion population sizes. This suggests that the effects of EPIC cannot be entirely ascribed to reduction of the number of trapped ions present during detection.

As mentioned previously, the initial motivation behind the application of the electron beam during detection was to investigate possible perturbations in the electrostatic fields and subsequent frequency shifts that may arise. Figure 3 illustrates the effect that the electron beam can have on the measured cyclotron frequency shift, as compared to that observed with non-EPIC experiments using different isotope peaks of bradykinin $[M + 2H]^{2+}$. This figure illustrates how the ion cyclotron frequency of the ion packet is shifting with time as it spins on its excited cyclotron orbit. With the traditional detection technique, it is

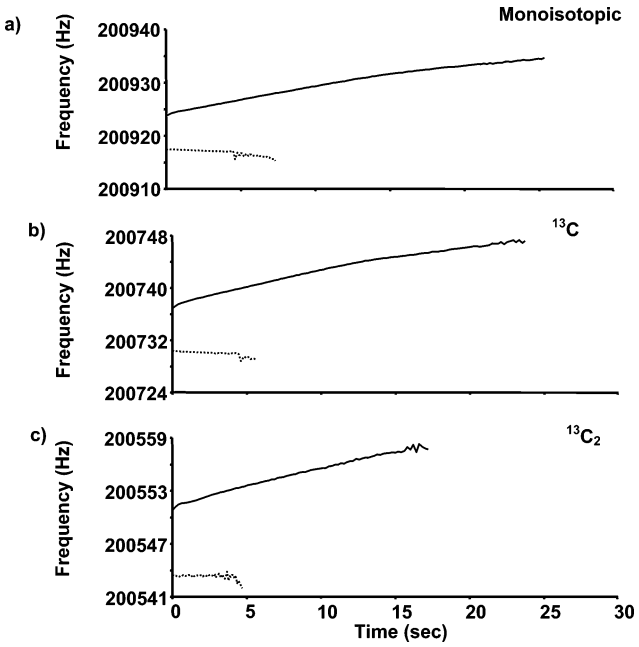

Figure 3. Bradykinin $[M + 2H]^{2+}$ was used to show that the frequency shift in time changes direction with the application of EPIC. The nonmodified detection technique (dotted line) slopes to a lower frequency with time, whereas the EPIC-produced signal (solid line) shifts to a higher frequency with time. (a) The frequency change for the monoisotopic *m/z* species. (b) The frequency shift for the $^{13}C_1$ isotope peak. (c) The frequency shift for the $^{13}C_2$ isotope peak. The higher magnitude peaks are detected for a longer period of time when comparing the monoisotopic peak in part a to the $^{13}C_2$ isotope peak in part c.

common to see the frequency shift to a lower value with time.[17,47] However, with the EPIC-produced signals, we observe the frequency shift to a higher value with time. One possible explanation for this observation is that when the electron beam is turned on, changes in the electrostatic field potentials inside the ICR cell are observed. The addition of the electron beam produces a radially inward-directed force on the positive ions and would thus be expected to shift the ICR frequency higher, lower *m/z*, even at time zero during detection, as observed in Figure 3. This figure shows the frequency shift with time to be much more prominent with the EPIC-produced spectra. In the resultant mass spectra of bradykinin (data not shown), the peaks produced from the EPIC signal are thus broader due to the cyclotron frequency drifting with time. However, this is not always the case; with careful optimization of the detection parameters, it is possible to nearly eliminate any frequency shift with time. Figure 4 shows the frequency shift with time of the different isotope peaks of substance P $[M + 2H]^{2+}$. Here, the frequency shifts with the non-EPIC results are greater and slope to a lower frequency with time with EPIC. The frequency with an EPIC-produced signal is relatively constant, in which the standard deviation of the detected frequency for the monoisotopic peak is 0.119 Hz over the 10-s detection period, whereas the standard deviation for a non-EPIC result is 1.4 Hz. This results in higher resolving power in the mass spectra, which are shown in Figure 5. In this figure, the observed resolving power (fwhm) increased from ~250 000 to ~850 000

(47) Guan, S.; Wahl, M. C.; Wood, T. D.; Marshall, A. G. *Anal. Chem.* **1993**, *65*, 1753−1757.

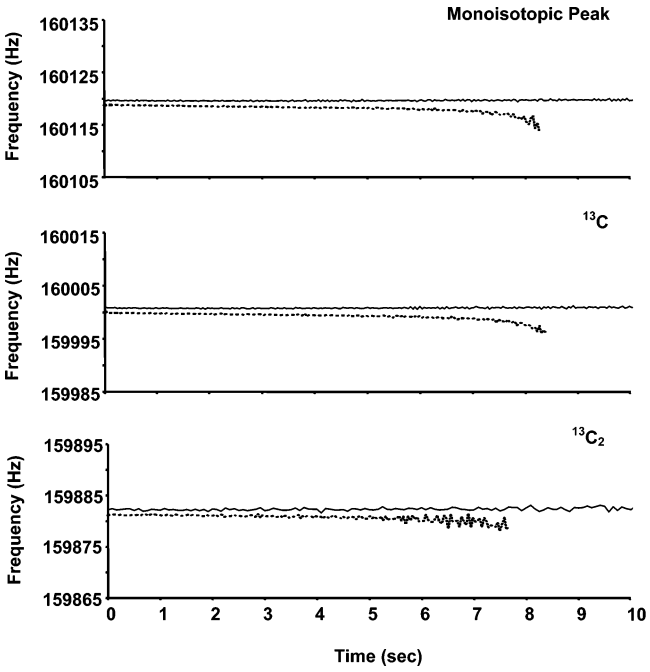

Figure 4. Plots of the shift in frequency for the different isotope peaks for substance P $[M + 2H]^{2+}$. The solid line is the result of the EPIC experiment. The dotted line is the non-EPIC result. The EPIC results produce less drift in frequency and yield a higher-resolution mass spectrum.

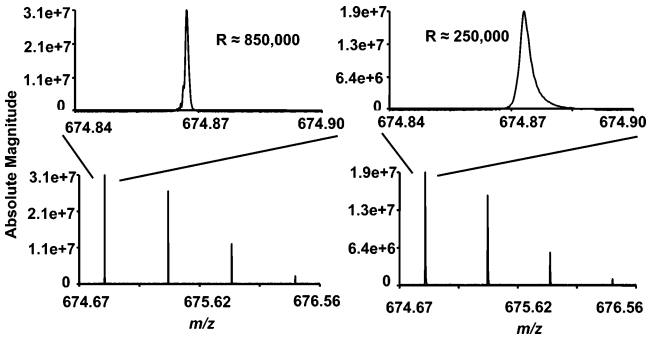

Figure 5. Mass spectrum of the substance P $[M + 2H]^{2+}$ without EPIC (right) and with EPIC (left). The inset spectra illustrate the observed monoisotopic peak and demonstrate improvement in resolving power by a factor of 3 with the application of EPIC.

with the application of EPIC. Data were collected over only a 10-s detection period. The non-EPIC signal decayed below the noise within that time frame (~8 s), while the EPIC signal was still ~15 times the noise level in the time-domain signal. It should be noted that even though the frequency drift was eliminated, which improved the resolving power in the previous example, no fine structure was observed. However, we are able resolve two closely spaced peaks with the application of EPIC. Figure 6 shows an example of the ability to observe fine structure in the bradykinin $[M + 2H]^{2+}$ peak that is 2 Da above the monoisotopic mass with EPIC utilization. This peak is composed of both ^{15}N and ^{13}C substitutions, and in this figure, the ^{15}N and ^{13}C peaks are resolved. The mass difference between ^{15}N and ^{13}C is 6.4 mDa and requires a resolving power of 165 000 to observe separation. The resolving power increased from ~90 000 to ~250 000 with application of EPIC, and fine structure is observed in the spectrum.

It is likely that increasing the potential applied to the heated cathode increases the number of electrons traversing the ICR cell.

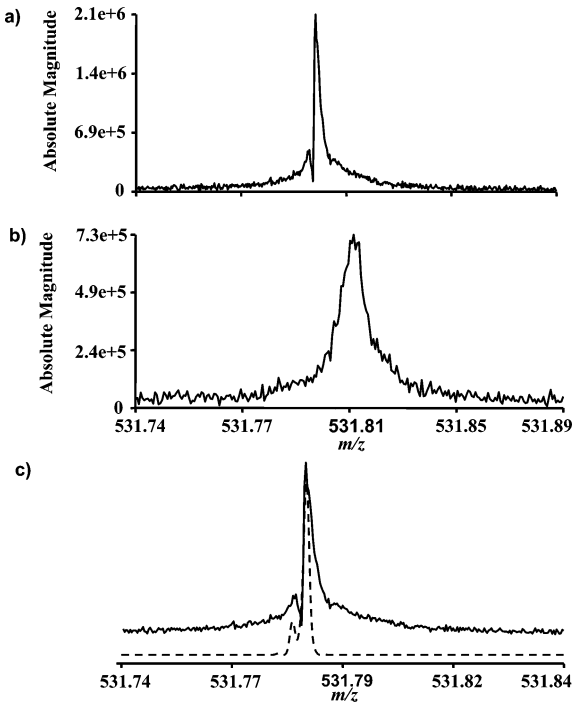

Figure 6. Mass spectra of the M + 2 isotope peak of Bradykinin $[M + 2H]^{2+}$ ions. (a) EPIC mass spectrum. The split in the peak results from the mass difference of ^{15}N and ^{13}C. (b) Mass spectrum from non-EPIC experiment; here, no fine structure is observed. (c) An overlay of the EPIC data (top, solid line) and the theoretical fine structure (bottom, dotted line).

It should be noted that applying a potential to the cathode surface in the absence of any cathode heating current resulted in no observed change in time-domain signal duration, as compared with non-EPIC results. Thus, cathode surface voltage itself is not directly contributing to the observed effects of EPIC. The number of electrons that enter the ICR cell is controlled by the cathode heating current and the bias voltage applied to the dispenser cathode. As the applied voltage increases, the number of electrons being sent through the ICR cell increases.

Application of EPIC is likely to result in alteration of the trapping electrostatic field potentials. Due to the high electron densities experienced, EPIC likely modifies potential fields in a manner similar to that of a solid electrode placed through the center of the ICR cell. Solouki et al.[48] previously implemented a Kingdon trap[49] to be used with ICR detection, which utilized a solid copper wire electrode placed on the central axis of the ICR cell to act as an ion guide and facilitate ion transfer from the source cell to the analyzer cell. The presence of this wire caused perturbations in electrostatic field lines of the trapping potentials. It is likely that there are similar shifts in the electrostatic field lines when there is a high-density electron beam present in the ICR cell, as encountered during EPIC experiments. The electron beam will produce a negative potential region through the center of the ICR cell. Gillig et al.[50] described the theoretical ion motion within this particular ICR cell design. When a negative potential is placed through the center of the ICR cell, the radial electric

(48) Solouki, T.; Gillig, K. J.; Russell, D. H. *Anal. Chem.* **1994**, *66*, 1583−1587.
(49) Kingdon, K. H. *Phys. Rev.* **1923**, *21*, 408−418.
(50) Gillig, K. J.; Bluhm, B. K.; Russell, D. H. *Int. J. Mass Spectrom. Ion Processes* **1996**, *157/158*, 129−147.

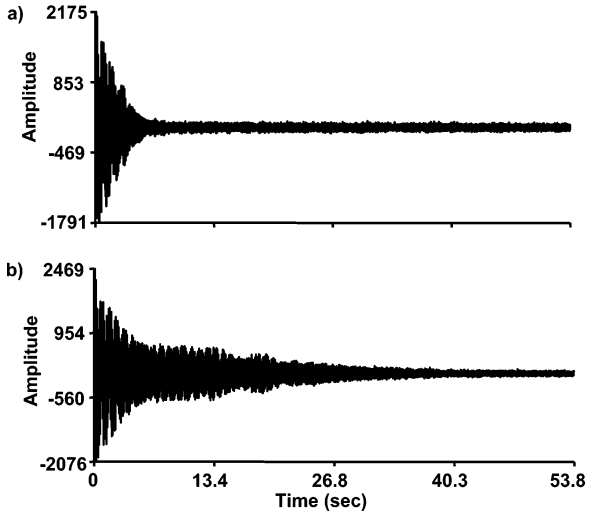

Figure 7. Successive time-domain signals for ubiquitin $[M + 6H]^{6+}$: (a) time-domain signal for the nonmodified detection technique and (b) EPIC-produced time-domain signal. The length of the detected ion signal increased by a factor of ~5 with the application of EPIC.

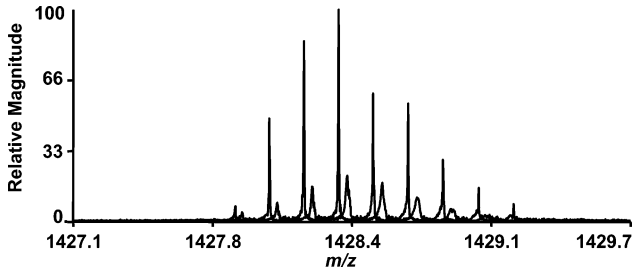

Figure 8. The mass spectra from the time-domain signals from Figure 7a and b. The two spectra are overlaid to show the increased resolution and sensitivity with the EPIC results.

field is directed inward for some volume of the ICR cell. Thus, the magnetron motion within this region will relax back toward the central axis of the ICR cell with time, with the presence of collisional damping. Potentially, EPIC experiments will present many advantages inherent in the cell design presented by Solouki et al. but will also allow flexibility in the time in which the "electrode" is present within the cell. However, the similarity of the axial electron beam to the actual Kingdon trap will depend on the extent to which the electron beam density is constant along the *z* axis of the ICR cell.

Another important point to consider is that increased time-domain signals are a prerequisite for high performance but do not always translate into improved resolving power. The time-domain signals in Figure 2a and b resulted in mass spectra of approximately equal resolving power, despite the much longer EPIC-produce result. However, under some conditions, it is possible to produce spectra of improved resolving power and sensitivity with EPIC. Figure 7 shows the time-domain signal produced with the ubiquitin 7^+ charge state. Figure 7a shows the non-EPIC control results, whereas Figure 7b illustrates the EPIC results. With the application of EPIC, the time-domain signal increases from ~8 to ~40 s, which is a factor of ~5 improvement. Figure 8 provides an overlay of the Fourier transformed time-domain signals of Figure 7a and 7b. The higher-magnitude, isotopic envelope of ubiquitin 7^+ observed with higher resolving power is the EPIC result, and the lower-magnitude, lower-performance spectrum is the result of the non-EPIC experiment. Figure 8 demonstrates that both longer time-domain signals and improved spectral resolving power are possible with EPIC. In the analysis of data in Figure 8, it was also noticed that as the two spectra are overlaid, the positions of the isotopic distributions do not match up exactly. This is not surprising, since the instrument was not calibrated with the electron beam turned on. The radial electric field is resultant from the applied trapping potentials and drives magnetron motion. The effect of turning on the electron beam changes the radial electric field and, thus, also changes the magnetron motion. Any change to parameters associated with the ICR cell will cause changes in the calibration of the instrument. To maintain the expected high mass measurement accuracy achievable with FTICR-MS, the calibration of the instrument needs to be performed with the electron beam turned on. Therefore, the mass measurement accuracy should not be compromised with the use of the electron beam.

The application of EPIC has also been observed to affect the phenomenon known as peak coalescence. Coalescence limits the number of ions that can be effectively contained and detected in FTICR experiments. Figure 9a depicts the time-domain signals for the 2^+ charge state of bradykinin in which closely spaced m/z species coalesce after a short time period. The resulting mass spectra show a small peak just to the right of the monoisotopic which is the result of peak coalescence. This was determined by segmenting the time-domain signal into two different regions. Figure 9b shows the first segment, which contains the first 1.15 s of the time-domain signal. This part of the signal contains information of different isotopes of bradykinin. Figure 9c shows the second segment, which contains the information from 1.25 to 16 s. The mass spectrum that results from this time-domain segment contains only a single m/z peak and no isotopic information. The appearance of this peak happens at the same time that all the isotopic peaks disappear. This collapse of isotopic peaks into a single peak is known as coalescence and serves as a limitation to FTICR performance. Figure 10 shows the EPIC produced time-domain signal and the resulting mass spectra under experimental conditions otherwise identical to those in Figure 8. With the application of EPIC, the coalescence is no longer observed. This observation was repeatable, because we were able to turn the electron beam on and off and see the appearance and disappearance of the peak coalescence. Under normal conditions, coalescence was observed with bradykinin $[M + 2H]^{2+}$; however, with the application of EPIC, peak coalescence was mitigated.

CONCLUSIONS

Factors which promote dephasing and degrade ion cloud phase coherence during detection can be substantially reduced by producing a high-density beam of electrons through the center of the ICR cell. The improved ion cloud stability can be observed by the increased length of the time-domain signal. The application of EPIC produces time-domain signals that are, on average, 3−5 times longer than non-EPIC results. Though resolution and mass accuracy are typically a function of time-domain signal length, the improved time-domain data sets taken with EPIC do not necessarily lead to improved resolution. However, under some of the experimental conditions we investigated, it is possible to obtain an increase in both resolution and sensitivity with EPIC. We

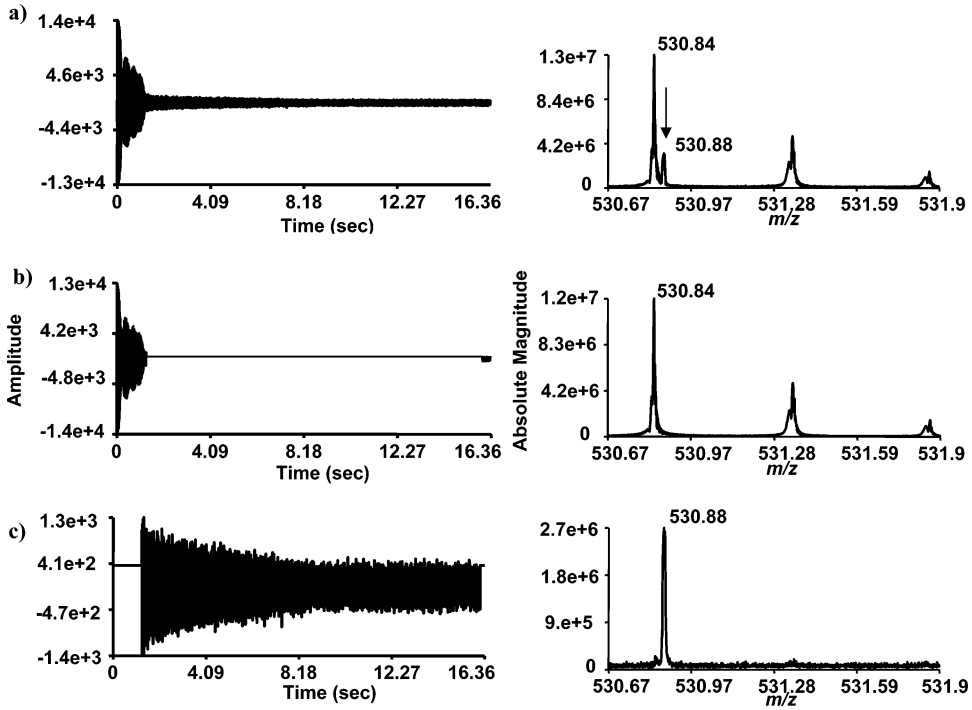

Figure 9. Peak coalescence. (a) The full time-domain signal and the resultant mass spectrum of bradykinin $[M + 2H]^{2+}$. The small peak to the right of the monoisotopic peak is the coalesced signal (marked by an arrow). (b) The first part of the time-domain signal is conserved, and all other data points are set to zero. The Fourier transform of the truncated time-domain signal yields a mass spectrum with an isotopic distribution of bradykinin 2^+, as would be expected. (c) The second part of the time-domain signal is conserved, while all data points in the first part are set to 0. The resultant mass spectrum yields a single peak, which is caused from the coalescence of the different isotope peaks of bradykinin 2^+.

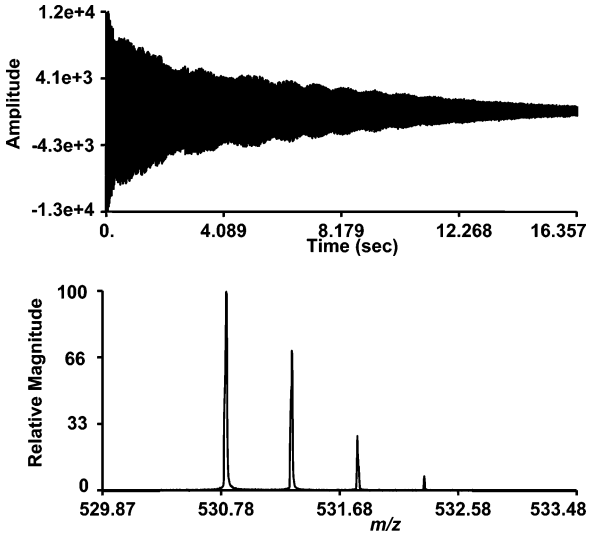

Figure 10. The time-domain signal and the resultant mass spectrum after application of EPIC under the same conditions that yielded peak coalescence shown in Figure 9. With EPIC, peak coalescence is eliminated.

demonstrate a factor of 3 improvement in resolution with the application of EPIC.

An additional interesting feature of the EPIC results is the observed effect that the electron beam has on the cyclotron frequency shift. The application of EPIC seems to cause the frequencies to shift to a higher value with time. Additionally, the application of EPIC can prevent closely spaced peaks from coalescing. The mechanisms underlying the electron beam effects on ion cloud motion that result in longer observed time-domain signals are not fully understood at present. However, this observation of increased time-domain signal is significant and should provide greater insight into ion motion and the effects caused by perturbations in the electric field within the ICR cell. Finally, it is likely that the application of EPIC, or a derivative of it, can be implemented in the future to exploit the unique enhancements that it provides.

ACKNOWLEDGMENT

This research was supported by the National Science Foundation, Instrument Development for Biological Research Program, Grant No. DBI-0352451; the Murdock Charitable Trust; and the National Institutes of Health Biotechnology Training Grant. The authors also thank Gordon Anderson for the data analysis tools (ICR-2LS) and Harold R. Udseth, Gökhan Baykut, and Eugene Nikolaev for helpful discussions.

Received for review April 10, 2005. Accepted July 19, 2005.

AC050606B